



EK2360 HANDS-ON MICROELECTROMECHANICAL SYSTEMS  
ENGINEERING

---

## Final Report

---

HINARD Killian  
HANGARD Kelyan  
COHEN-DUMANI Joshua  
OH William

Group 1

July 3, 2023



# Contents

<b>1</b>	<b>Introduction</b>	<b>2</b>
<b>2</b>	<b>Design Schematics</b>	<b>2</b>
2.1	Design 1A . . . . .	2
2.2	Design 1B . . . . .	2
<b>3</b>	<b>Actuation Mechanism</b>	<b>2</b>
3.1	Actuation Force . . . . .	2
3.2	Lateral Stability . . . . .	4
<b>4</b>	<b>Restoring Mechanism</b>	<b>6</b>
4.1	Primary restoring mechanism . . . . .	6
4.1.1	Design . . . . .	6
4.1.2	Longitudinal Stiffness . . . . .	6
4.1.3	Horizontal stiffness . . . . .	7
4.2	Second restoring mechanism . . . . .	7
4.2.1	Stiffness of second mechanism . . . . .	7
4.3	Rotational Stability . . . . .	7
4.3.1	Primary Design . . . . .	8
4.3.2	Secondary Design . . . . .	8
<b>5</b>	<b>Locking Mechanism</b>	<b>8</b>
5.1	Implementation on our Designs . . . . .	8
5.2	Design Parameters . . . . .	9
5.3	Deformation of the Beam in the Pull-In Position . . . . .	10
<b>6</b>	<b>Fabrication Phase</b>	<b>10</b>
<b>7</b>	<b>Evaluation Phase</b>	<b>11</b>
7.1	Measurements . . . . .	11
7.2	Design expectations and failure analysis . . . . .	13
7.3	Recommendations for a future cycle . . . . .	13
<b>8</b>	<b>Conclusion :</b>	<b>13</b>

# 1 Introduction

For the course EK2360 Hands-on MEMS Engineering we had to create a MEMS device capable of inserting or removing a micro-mirror from a X-crossing of the optical path of optical fibers. This device was to move laterally (in-plane) when voltage was applied and be able to lock in its full-in and full-out position. For the fabrication of this device we went through a design phase where we calculated the dimension of our actuator, of the restoring mechanism and our locking mechanism. We then verified our result using simulations on COMSOL. Then we fabricated the devices in clean rooms in Kista. Finally we evaluated our devices to compare with the expected results and we tried to explain and identify our failures to find what we could change in a future cycle.

## 2 Design Schematics

### 2.1 Design 1A

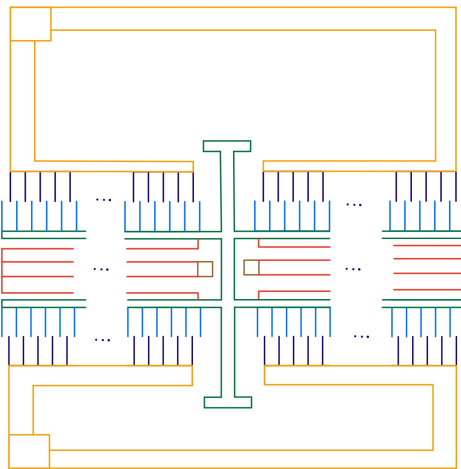


Figure 1: Our primary design

In figure 1 we have the schematic of our primary design with the anchor points of our springs situated inside the mechanism (The springs are drawn in red and the anchor points in brown).

### 2.2 Design 1B

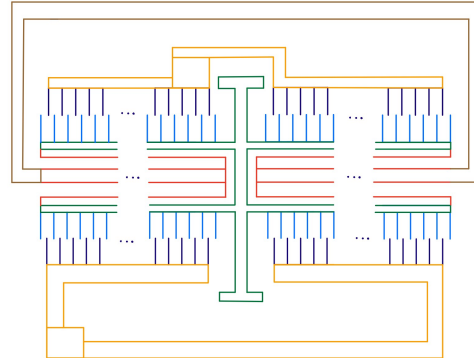


Figure 2: Our secondary design

In figure 2 we have the schematic of our alternative design with the anchor points of our springs situated outside the mechanism.

## 3 Actuation Mechanism

### 3.1 Actuation Force

We must now define the various geometric parameters of our system.

**Value of V :** To begin, we must decide the value of the voltage to apply to move our actuator to its final positions. We know that the maximum voltage that we apply to our electrodes is  $V_{max} = 65V$ . Seeing no reason not to take advantage of this, we will use a voltage of 65V.

**Value of w :** We now need to determine the dimension  $w$  (finger width). The only constraints which we have concerning the choice of  $w$  are that it is necessary to minimize this one in order to minimize the total length of the actuator, and the manufacturing processes impose on us a minimum dimension of  $4 \mu m$ . We have therefore chosen to take  $w = 4 \mu m$  to satisfy these two constraints.

**Value of g :** For the value of  $g$  (the distance between each finger) we have in the same way as for  $w$ , only two constraints allowing us to choose a suitable dimension. We must minimize  $g$  so as to increase the force produced by the actuator, and we must also respect a minimum  $g$  of  $3 \mu\text{m}$  which corresponds to a manufacturing constraint. We have therefore chosen, following the same logic as for  $w$ ,  $g = 3 \mu\text{m}$ .

**Value of h :** The area where the actuator can be used is the constant force range. Using the graphics in the slides, we can give a first estimate that (for  $30\mu\text{m}$  fingers), the force is more or less constant between 5 and 65% of the total finger length. In our design we want a displacement of  $15 \mu\text{m}$  so we would need a theoretical finger length of at least  $25 \mu\text{m}$  ( $\text{length} = \frac{15}{0.6}$ ). So we have chosen  $h = 25 \mu\text{m}$ .

**Value of N :** The last parameter to be determined is  $N$ , the number of fingers of our comb-drive actuator. To do this we know that we must have a minimum force of  $30 \mu\text{N}$ . Moreover we know that the force of the actuator in the region of constant operation of this one is given to us by:

$$F \approx \epsilon_0 N \frac{hV^2}{g}$$

so we have :

$$N = \frac{Fg}{\epsilon_0 h V^2}$$

by doing the numerical application we finally find  $N$  must be at least 96. Based on simulations, and space on the chip, we choose to have 104 comb fingers. This gives us a theoretical force (in the constant force region of the actuator) of  $32.37 \mu\text{N}$ .

As we can see from figure 3, the simulated force more or less matches the theoretical result. There are some values of the overlap (in the constant force region) for which the force does not appear constant, but we can probably disregard

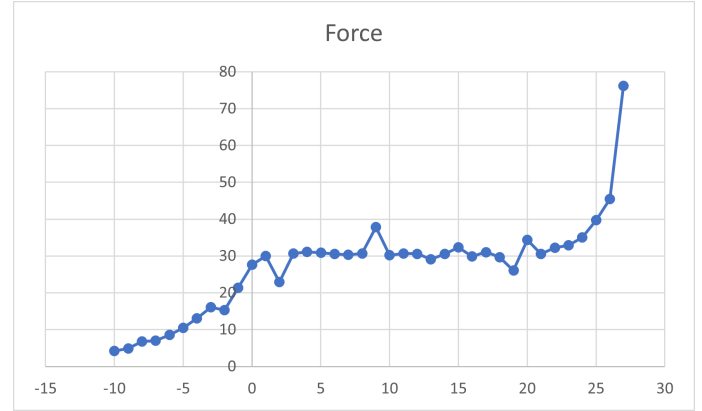


Figure 3: Graphic of the force plotted according to how much overlap there is.

these simulated discrepancies as the average force in this region is above the  $30 \mu\text{N}$  minimum.

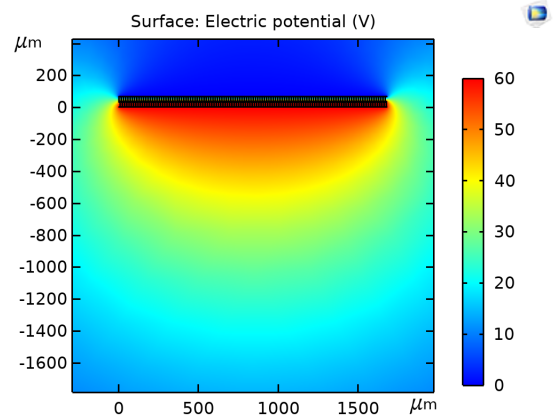


Figure 4: Simulation of the comb drive

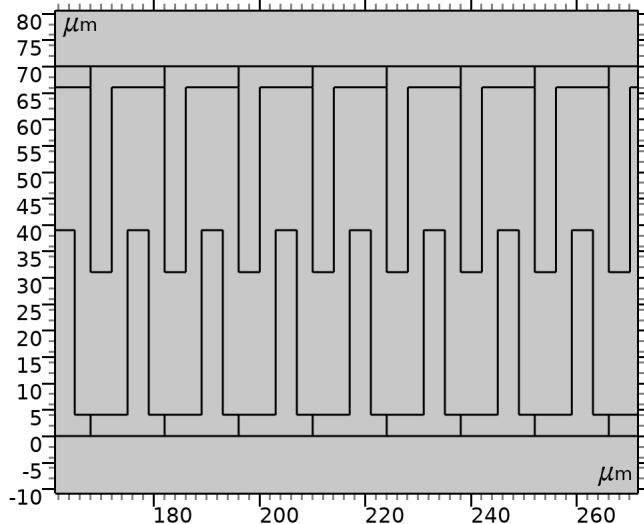


Figure 5: Fingers of the comb drive

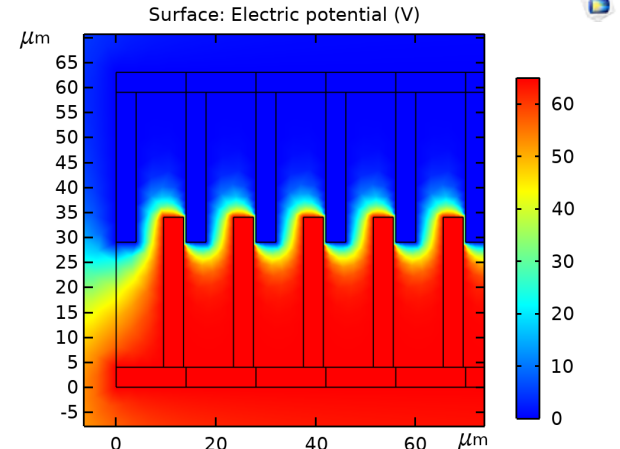


Figure 7: Electric potential with a large horizontal displacement

Name	Expression	Value	Description
w	4e-6[m]	4E-6 m	height of comb drive base
t	25e-6[m]	2.5E-5 m	out of plane
height	35e-6[m]	3.5E-5 m	height of finger
free	10e-6[m]	1E-5 m	free space between two f...
overlap	8e-6[m]	8E-6 m	overlap between fingers
V0	60[V]	60 V	
ovmax	16.25[um]	1.625E-5 m	max overlap
ovmin	1.25[um]	1.25E-6 m	min overlap
nb	120	120	nb of fingers
cushion_x	20*nb[um]	0.0024 m	
cushion_y	25*nb[um]	0.003 m	

Figure 6: Parameters of our comb drive

### 3.2 Lateral Stability

To calculate the lateral stability of the actuator we first need to calculate the lateral stiffness of our spring designs. Since the actuation mechanism is the same for both designs, we only need to calculate the force once. The lateral stiffness of our primary mechanism is  $k_x = \frac{\text{force}}{\text{displacement}} = \frac{30 \times 10^{-6}}{5.8476 \times 10^{-9}} = 5130.3 \frac{N}{m}$ . Using these spring constants, we can evaluate the stability of our systems by calculating the force for different values of lateral displacement (up to close to the initial gap value), using the simulation on COMSOL.

Exporting the data to excel and plotting the

electrostatic force and the spring restorative force when the overlap is equal to 20  $\mu\text{m}$  gives us the graph seen in figure 8. As we can notice, the spring restorative force is much larger than the electrostatic force. this can be further confirmed with the data visualized on fig 9. As we can see, there is still a sizeable difference, even with a displacement of 2,6  $\mu\text{m}$ .

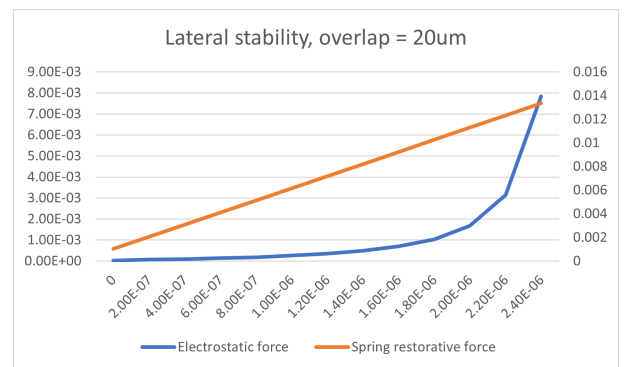


Figure 8: Lateral stability of our primary design for a 20um overlap, left axis is the ES force and secondary axis the spring force.

We also considered the lateral stability for an overlap of 5  $\mu\text{m}$  using the same method. Our results can be observed on figure 10. As we can see, the difference is even more pronounced and there

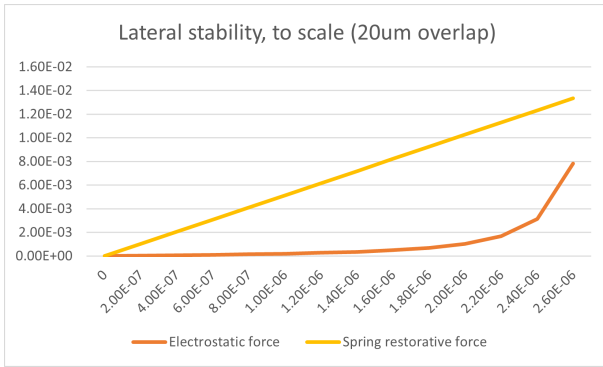


Figure 9: Lateral stability of our primary design for an overlap of  $20 \mu\text{m}$ , on the same scale

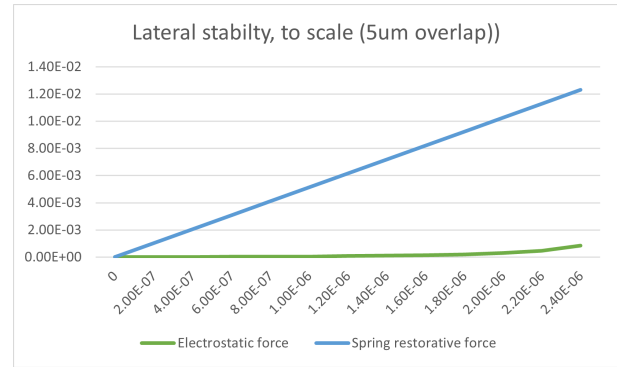


Figure 11: Lateral stability of our primary design for an overlap of  $5 \mu\text{m}$ , on the same scale

is a factor of 16 with the maximum overlap. We can therefore pretty safely infer that our primary design will remain stable during general use, and that the lateral stability is not a big cause of concern.

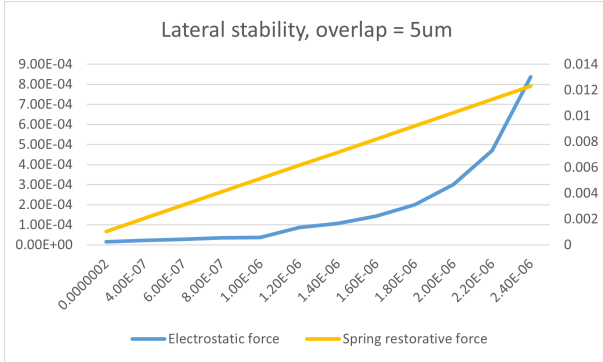


Figure 10: Lateral stability of primary design for an overlap of  $5 \mu\text{m}$ , left axis is the ES force and secondary axis the spring force

For our secondary design, we have considered the lateral stability, taking into account the fact that the spring constant of our second design is  $3675,93 \text{ N/m}$ . We get the following graphics :

From these graphics we can fairly infer that lateral stability will not be a problem during regular use of the mechanism. There might however be a problem if we have very large lateral displacements, such as ones greater than  $2,8 \mu\text{m}$ , and at large overlap.

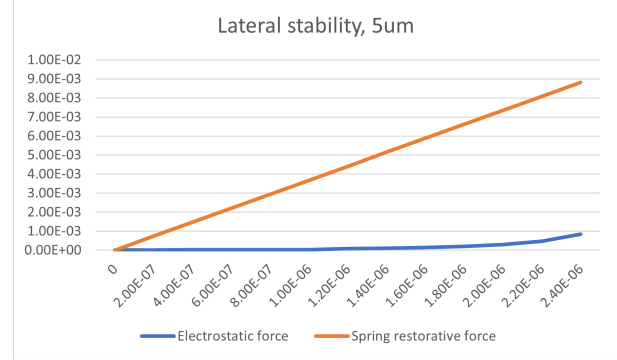


Figure 12: Lateral stability of our secondary design for an overlap of  $5 \mu\text{m}$ , on the same scale

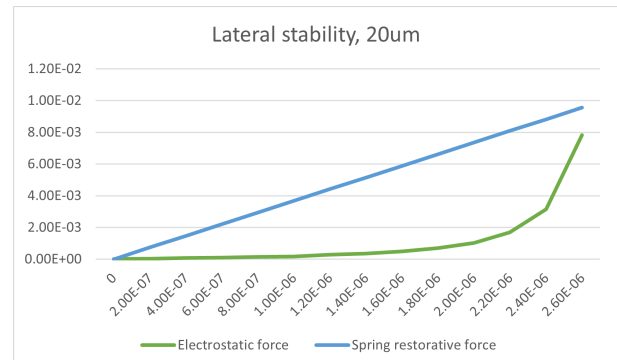


Figure 13: Lateral stability of our secondary design for an overlap of  $20 \mu\text{m}$ , on the same scale

## 4 Restoring Mechanism

### 4.1 Primary restoring mechanism

#### 4.1.1 Design

We designed our primary restoring mechanism using springs made of 2 folded cantilever beams with anchor points situated symmetrically to either side of the central moving part of the mechanism.

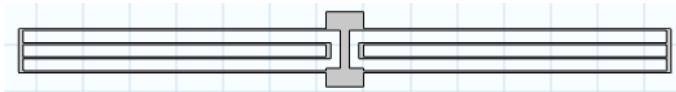


Figure 14: Restoring mechanism on COMSOL

#### 4.1.2 Longitudinal Stiffness

Our system (shown in Figure 15) is composed of 4 springs in parallel with the stiffness constant

$$k_0 = \frac{EWT^3}{2L^3} \Rightarrow k_{eq} = \frac{2EWT^3}{L^3} \quad (1)$$

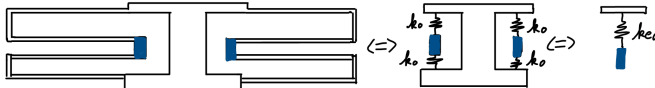


Figure 15: Calculation of the stiffness constant

We want the passive restoring force in each end position to be  $F_{res} = 30\mu N$  and the total displacement between the two end positions to be  $30 \mu m$ . Then the spring constant must be:

$$k_{eq} = \frac{F_{res} \cdot 2}{\text{total displacement}} = 2 \quad (2)$$

$$\frac{2EWT^3}{L^3} = 2 \quad (3)$$

$$\frac{WT^3}{L^3} = 5.88 \cdot 10^{-12} \quad (4)$$

Then we can choose our parameters as:

- $W = 25\mu m$

- $T = 4\mu m$

- $L = 652\mu m$

We simulated the force over the displacement of the system with COMSOL by applying a downwards force at the center of our model. The results can be visualized on figures 16 and 17.



Figure 16: COMSOL simulation of the restoring mechanism in the wanted direction

We then get these results for the dimensions calculated previously :

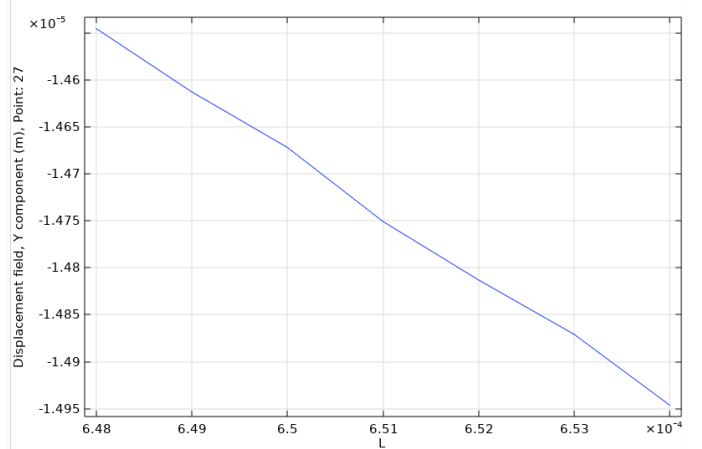


Figure 17: Force over the displacement of the system

We can then compute the stiffness constant:

$$k_y = \frac{F}{\text{displacement}} \quad (5)$$

$$k_y = \frac{30 \cdot 10^{-6}}{14.813 \cdot 10^{-6}} \quad (6)$$

$$k_y = 2.025 N/m \quad (7)$$

#### 4.1.3 Horizontal stiffness

We find the stiffness in the horizontal direction by applying a horizontal force in our simulation and dividing by the displacement created.

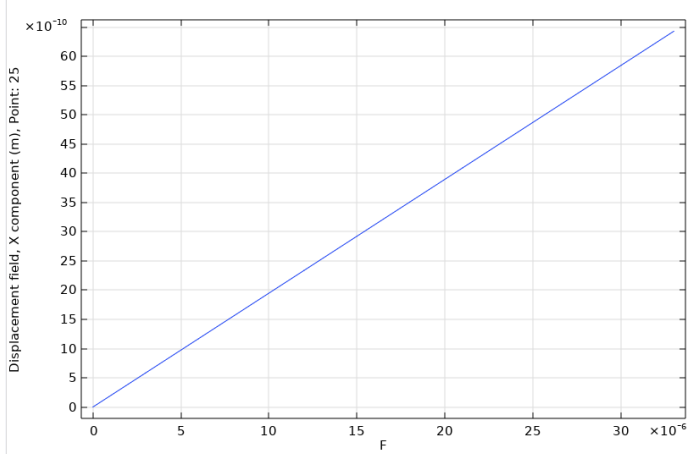


Figure 18: Simulation of the displacement in function of the force in the unwanted direction

We can then find the stiffness constant:

$$k_x = \frac{F}{\text{Displacement}} = \frac{30 \times 10^{-6}}{5.8476 \times 10^{-9}} = 5130.3 \quad (8)$$

$$\text{So } \frac{k_x}{k_y} = \frac{5130.3}{2.025} = 2533.48$$

The stiffness in the unwanted direction is 2533.48 times bigger than in the wanted direction, which is good and likely will lead to good stability.

#### 4.2 Second restoring mechanism

For our second restoring mechanism we choose to also use 2 folded cantilevers but with the anchor points situated on the exterior of the mechanism.

##### 4.2.1 Stiffness of second mechanism

This second mechanism being also constructed with 4 springs in parallel should have the same constant in the y direction  $k_y$  than the previous mechanism but a different stiffness. We verify those assumptions by simulation.

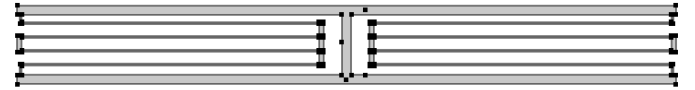


Figure 19: Second design with exterior anchor point

We proceed in the same way as for the first mechanism :

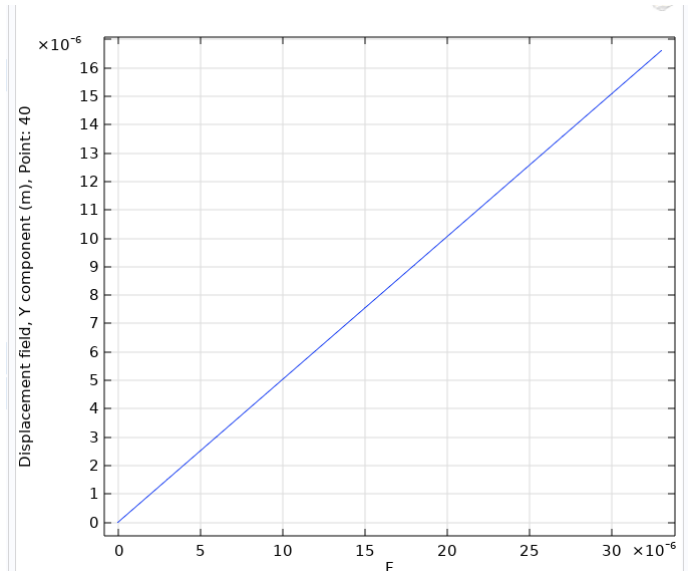


Figure 20: Displacement in function of force in wanted direction

$$k_y = \frac{F}{\text{Displacement}} = \frac{30 \times 10^{-6}}{15.103 \times 10^{-6}} = 1.9863 \quad (9)$$

We also have :

$$k_x = \frac{F}{\text{Displacement}} = 3675.93 \quad (10)$$

#### 4.3 Rotational Stability

For the rotational stability we use COMSOL to find the rotational spring constant in the out-of-plane direction. We do this by applying 2 force of

opposite direction at the 2 extremities of the central moving structure. This creates a torque that induces a certain rotation. Then by knowing the force applied we can find the rotational stiffness.

#### 4.3.1 Primary Design

The results of this analysis for our primary design can be found on figures 21 and 22.

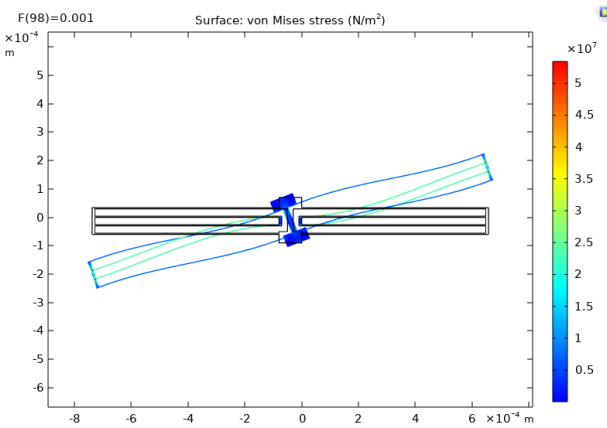


Figure 21: Exaggerated rotational stress of our primary design

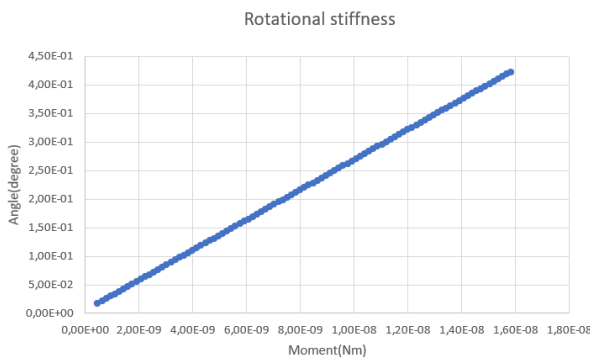


Figure 22: Rotational stiffness of our primary design

From those graphics we can deduce the rotational stiffness:

$$k_{rotational1} = 37.8 \cdot 10^{-9} \text{ degree/Nm} \quad (11)$$

This complies to the constraint of  $k > 10 \cdot 10^{-9} \text{ degree/Nm}$  given in the task description in a satisfactory manner.

#### 4.3.2 Secondary Design

We proceed in the same way and get :

$$k_{rotational1} = 11.7 \cdot 10^{-9} \text{ degree/Nm}$$

The constraint  $k > 10 \cdot 10^{-9} \text{ degree/Nm}$  is also respected.

We note that our first design has a rotational stiffness about 3 times bigger than our second design. We can then conclude that the first design is a restoring mechanism more adapted to our needs.

## 5 Locking Mechanism

### 5.1 Implementation on our Designs

Our locking mechanism is implemented by a parallel plate actuator, used in digital mode. The design is shown in figure 23. The way it is then implemented into our primary design is shown on figure 29, and the implementation on our alternative design is shown on figure 30. While the actuator is in use, the locking electrode will be set to 65V, putting the actuator in the pull in position. The moving parts are shown in green. In the end positions, the rigid cantilever will keep the moving part in place.

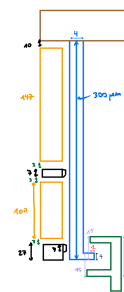


Figure 23: locking mechanism

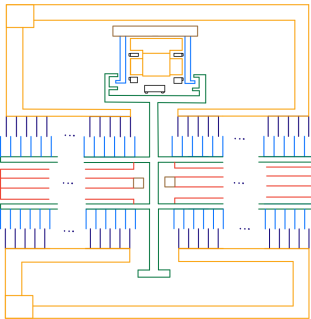


Figure 24: Locking mechanism on our main design

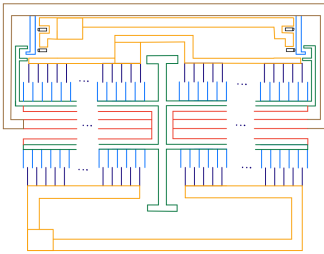


Figure 25: Locking mechanism on our alternative design

## 5.2 Design Parameters

In order to make sure that we are in digital mode, we need  $V_{pull-in} \leq 65V$ , and also ensure that the cantilever does not touch the electrode when we are in the pull in position.

The pull-in voltage for a cantilever is given by the formula from the lesson 1:

$$V_{pull-in} = \sqrt{\frac{8kd^3}{27\epsilon_0 A}} \quad (12)$$

We choose to have a cantilever of Length  $L = 300\mu m$ . The area of the electrode is  $246\mu m \times 25\mu m = 6150\mu m^2$ . We consider the stiffness of the cantilever for  $L = 268\mu m$  (The point that get the closest to the electrode, see figure 26) The width of the cantilever is  $W = 25\mu m$

Then

$$k = \frac{EWT^3}{L^3} = 14.13 \quad (13)$$

Meaning that  $V_{pull-in} = 45.56V$ .

Verifying by simulation :

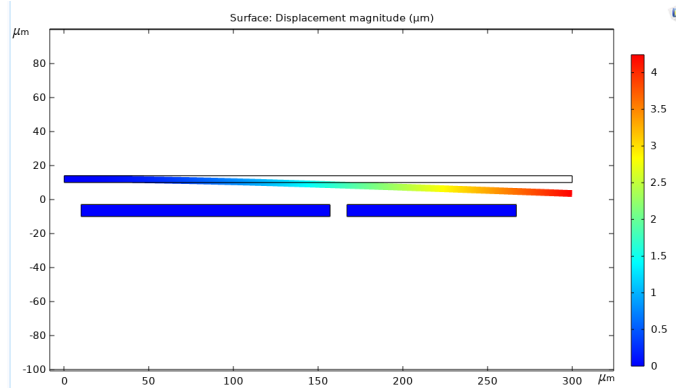


Figure 26: Simulation of the cantilever displacement on COMSOL with the electrode as implemented in our design

The cantilever is represented as the top block and the electrode are in blue.

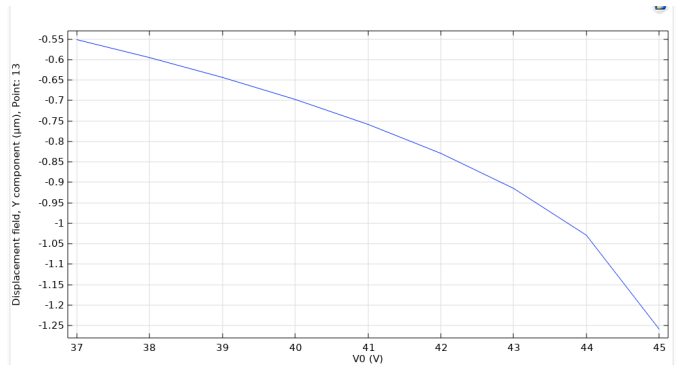


Figure 27: Graphical simulation of the cantilever displacement with the electrode as implemented in our design

We see that the pull in voltage is situated at a displacement of  $1/3$  of the distance which correspond to a displacement of  $1 \mu m$ . Graphically we can see that the pull in is around  $V_0 = 43.7$ .

The result in simulation is close to the one calculated analytically so we can conclude that the dimension chosen satisfy the condition  $V_{pull-in} \leq 65V$ . However we see that the pull in voltage in the simulation is less than the one calculated theoretically that is because We considered the stiffness  $k$  at the end of the cantilever and not how it varies along the beam. Also we didn't consider the fact that we have a gap in the electrode to leave space for the stoppers. This is shown on figure 26

### 5.3 Deformation of the Beam in the Pull-In Position

To simulate the worst case scenario we consider that the whole of the cantilever is in the pull-in position, ie that the gap between the electrodes and the cantilever is  $2 \mu\text{m}$ . Then we fix the cantilever in the position where it would touch the blockers.

By simulation we get :

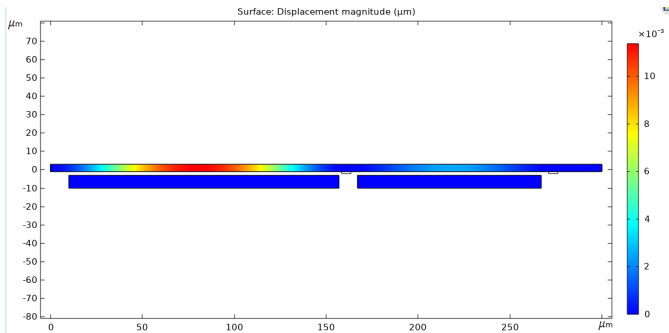


Figure 28: Deformation with blockers

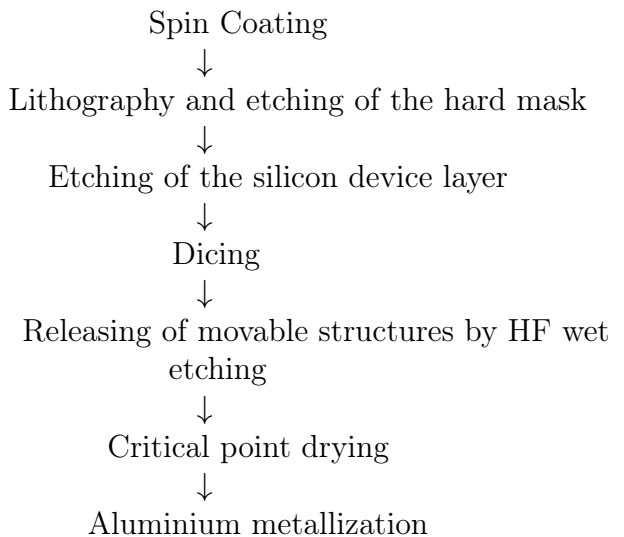
This is the simulation with an applied voltage of  $500V$  and we see that the maximum deformation in the cantilever is about  $10 \text{ nm}$ . On this simulation the cantilever is fixed between the two electrodes in blue and to the right of the right-most electrode. The cantilever is on top and the electrodes are on the bottom.

We showed the simulation for  $V_0 = 500V$  because in the case  $V_0=65V$  the displacement is

barely visible (around  $1 \text{ nm}$ ). In conclusion we see that there is no risk of the cantilever touching the electrodes and creating a short circuit.

## 6 Fabrication Phase

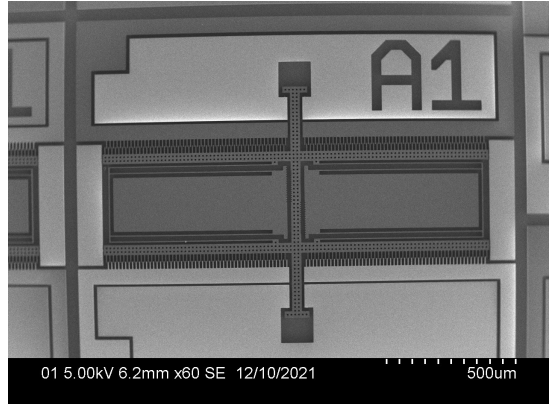
The process steps of the fabrication phase are described as follows:



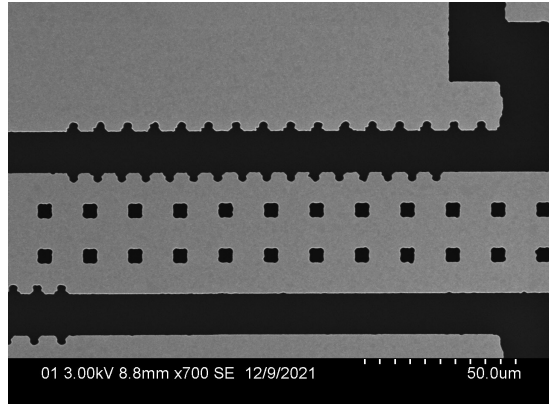
We were then able to visualize the results and take pictures using the SEM. The images of our A design can be seen on figure 29, and the design B on figure 30.

We were also able to notice using the SEM that our locking mechanism would not function properly. Indeed, the lockers were too far away from the parallel plate actuator, and it would not lock the mechanism in resting position. This was confirmed during the evaluation phase.

We were also able to get 3D images during the fabrication phase. This allowed us to see that (at least on this version) there was stiction. It was confirmed during the evaluation phase that most of versions also had stiction.



(a) Full picture of design A1



(b) Ruler system for evaluating displacement, primary design

Figure 29: Design A

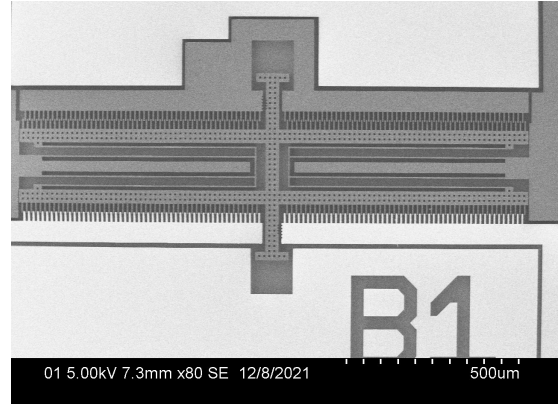
## 7 Evaluation Phase

### 7.1 Measurements

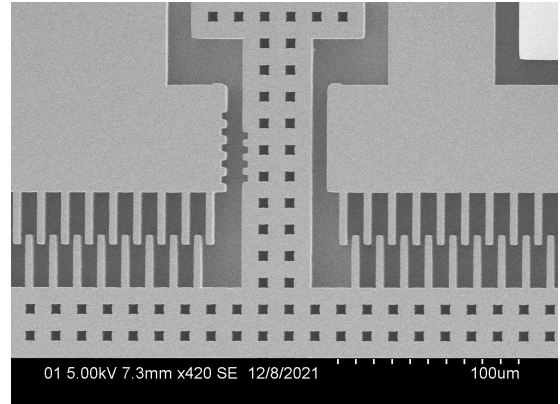
We first measured the displacement when varying the voltage using our ruler. Our measurements for our design A and B can be found in tables 1 and 2 respectively.

Applied Voltage	Displacement
15V	2 $\mu$ m
30V	4 $\mu$ m
45V	8 $\mu$ m
60V	15 $\mu$ m

Table 1: Measured displacement, design A



(a) Full picture of design A1



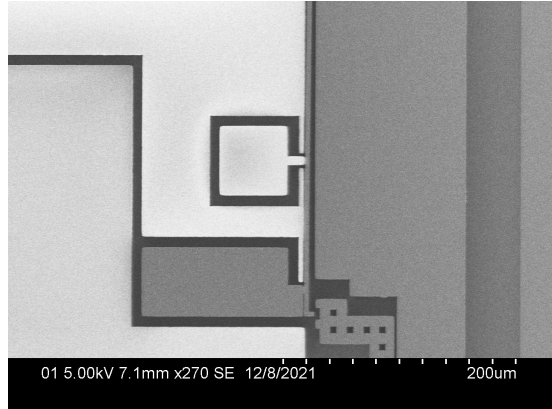
(b) Ruler system of our secondary design

Figure 30: Design B

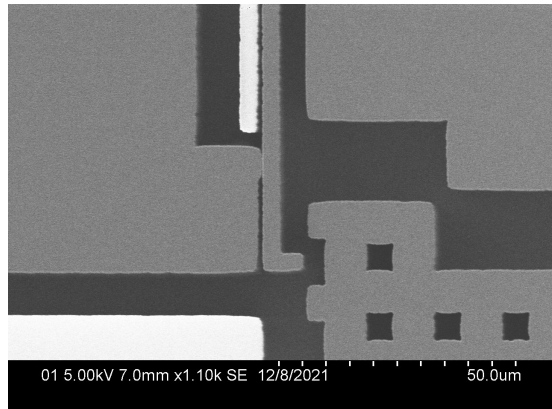
15V	1.5 $\mu$ m
30V	4.5 $\mu$ m
45V	8 $\mu$ m
55	12 $\mu$ m
60V	15 $\mu$ m

Table 2: Measured displacement, design B

First of all we noticed that the MEMS started moving directly when we started to apply a voltage even if the voltage was very low. Our simulations estimated that we would get a displacement of around 15  $\mu$ m for an applied voltage of 65V (14.813  $\mu$ m and 15.103  $\mu$ m for designs A and B respectively). In our results we noticed that we reach the 15  $\mu$ m value a bit earlier, at around 60V. From this we can deduce that our spring constant is a bit smaller than anticipated, which



(a) Our locking mechanism



(b) Zoom on the stopper

Figure 31: Locking mechanism



Figure 32: Visualizing stiction using the clean room 3D microscope

is not a problem for our requirements, since basic functionality is guaranteed. We also found the different pull-in/hold voltages of our design. For our primary design, The pull-in of our comb-drive

(undesirable) was at around 70V, and it was at around 68V for our secondary design.

**Lateral and rotational stability** To evaluate the lateral stability of our systems we pushed the center of one of our design with a probe in the unwanted direction. We pushed until the system was blocked by its lateral stoppers then released. Then we observed that for all our design the mechanism went back to its original position and was still functional.

To evaluate the rotational stability of our systems we pushed laterally on the tip of our system to induce a rotational motion. We pushed until the system was blocked by its lateral stoppers then released. Then we observed that for all our design the mechanism went back to its original position and was still functional.

We took video for the lateral and rotational stability.

**reproducibility of actuation** Most of our devices had stiction and didn't even move mechanically and those that moved mechanically didn't always move electrostatically. However our devices which did move electrostatically could go in both direction (push and pull) and we didn't observe the charging effect.

**Locking mechanism** The basic functionality of our locking mechanism weren't satisfying as the L shape hook at the end of the mechanism wasn't long enough and didn't properly lock the system.

Nonetheless our locking mechanism worked electrostatically with a pull-in voltage of 55V which respect our requirements. By calculation we had predicted a pull-in voltage of 45.56V and a pull in of 43.7V predicted by simulation,

**Reproducibility :** Most of the locking mechanism that didn't have stiction worked electrostatically and repeatedly.

**Note :** we didn't take the leak current into account because it always stayed constant at a value of 0.005 mA whatever the value ouf our voltage so we thought they might be a problem with the Ammeter.



## 7.2 Design expectations and failure analysis

While evaluating our designs, we found that, generally speaking, our designs are close to being functional. One critical error was the locking mechanism design, since the dimensions of our lockers in practice did not allow the parallel plate to be held in place, thus we could not lock the system in place. This could be due to negligence of fabrication tolerances, which we did not take into account. This is easily fixed by making the locks longer.

Another issue was the amount of mechanisms which were not functional due to stiction. From the  $\approx 120$  devices we tested, around 60% were non-functional, around 25% moved when pushed mechanically but did not work electrostatically, and around 15% were functional electrostatically. The high level of stiction could be due to various errors during the fabrication process, or to design flaws which led to our design being non-robust. It likely is a combination of both, as there are likely many ways in which our design could be made more robust. The 25% that only worked mechanically are particularly interesting as they highlight that there are likely spots where there were short-circuits. This could be due to the design rules followed, or errors in fabrication.

From the devices that worked electrostatically, we found that the various predicted values from simulations (pull-in voltages, displacement, stability) were largely correct, and the actual MEMS devices had more or less the same characteristics as planned. The small variations that we observed likely derive from small inaccuracies during fabrication, such as wet etching time, precision of the machines, etc.

## 7.3 Recommendations for a future cycle

In a future cycle, there are several details that would need to be changed. Our locking mecha-

nism should obviously be changed so as to become functional, increasing the length of the horizontal lockers and requiring less precision.

We could also find various ways to improve our design, perhaps changing the design rules to increase even more the robustness. We could also be more careful with the MEMS as it is pretty certain that some broke due to movement/dust (we were in a simple lab room for the evaluation lab, so there were likely some large dust particles).

We would also need to find ways to reduce the chance of short-circuit. This could be done by leaving larger gaps in some areas.

## 8 Conclusion :

This project was our first experience working on MEMS. It was very interesting as we participated in every process necessary to get a functional MEMS device. From the design to the fabrication and finally the evaluation of our device. We also learned how to use new softwares such as COMSOL and Klayout which will probably be useful in our future engineering career. Overall we believe this project was an enriching experience as we learned lots of